Research Article

Libing Qin, Zhong Xu*, Qingfeng Liu*, ZhiJie Bai, Chunjian Wang, Qiang Luo, and Yuan Yuan

Experimental study on mechanical properties of coal gangue base geopolymer recycled aggregate concrete reinforced by steel fiber and nano-Al_2O_3

https://doi.org/10.1515/rams-2023-0343
received November 01, 2022; accepted June 27, 2023

Abstract: Using recycled aggregates to prepare geopolymer concrete plays an essential role in reducing dependence on natural resources and solving the problem of waste accumulation. However, the application of geopolymer recycled aggregate concrete (GRC) has been greatly limited due to the defects in the quality of recycled aggregates and the limitations of the brittleness of concrete materials. Therefore, the work is dedicated to improving GRC properties and exploring the mechanism of action of steel fiber (SF) and nano-Al_2O_3. In this study, calcined gangue, slag, fly ash, and recycled aggregate were used as raw materials, the influence of SFs (0–1.25 vol%) was first explored by single factor analysis, and on this basis, the effect of nano-Al_2O_3 (NA) (0–2 wt%) on the GPC performance of SF was studied. The microstructure of GRC was analyzed by scanning electron microscopy. The test results showed that adding SF could significantly improve the splitting tensile and flexural strength of GRC, among which 0.75 vol% is the most excellent. However, the increase in compressive strength could be more apparent. The addition of NA can make up for the lack of SF in improving compressive performance. When NA content is 1 wt%, the version of GRC is most apparent. Adding 1% NA has the most significant advance in GRC performance. The microstructure analysis showed that the NA could promote the polymerization reaction, generate more gel, and make the contact interface between SF and matrix more compact, thus improving the strength of GRC.

Keywords: coal gangue, recycled aggregate, nano-Al_2O_3, steel fiber, microstructure

1 Introduction

With the growth of the global population and the acceleration of urbanization, the contradiction between a large number of civil engineering construction and the deteriorating ecological environment objectively promotes the development of the construction industry towards high efficiency, high performance, and sustainability. Ordinary concrete uses Portland cement as the main cementitious material, and its application has laid a solid foundation for developing the modern construction industry. However, every 1 ton of Portland cement produced will produce 0.55–0.95 tons of CO_2 [1]. With the increasing demand for it, the environmental issues brought about by its production process are becoming increasingly apparent. Seeking high-performance and more environmentally friendly green cementitious materials has become essential for developing concrete technology.

Geopolymer, proposed by Joseph Davidovits in 1978, is a new polymer material with a particular inorganic polycondensation three-dimensional oxide network structure [2]. It is a sustainable green engineering material with the advantages of a wide source of raw materials, less environmental pollution, good mechanical properties, and durability [3,4]. Many scholars regarded geopolymer as a potential substitute

* **Corresponding author: Zhong Xu,** State Key Laboratory of Geohazard Prevention and Geoenvironment Protection, College of Environment and Civil Engineering, Chengdu University of Technology, Chengdu 610059, China, e-mail: xzcdut@163.com
* **Corresponding author: Qingfeng Liu,** State Key Laboratory of Geohazard Prevention and Geoenvironment Protection, College of Environment and Civil Engineering, Chengdu University of Technology, Chengdu 610059, China, e-mail: liuqingfeng1@stu.cdut.edu.cn
Libing Qin: School of Civil Engineering, Southwest Jiaotong University, Chengdu 610031, China; State Key Laboratory of Geohazard Prevention and Geoenvironment Protection, College of Environment and Civil Engineering, Chengdu University of Technology, Chengdu 610059, China; Engineering Technology Research Center, Sichuan Mingyang Construction Engineering Management Co. Ltd., Chengdu 610017, China
ZhiJie Bai, Chunjian Wang, Yuan Yuan: State Key Laboratory of Geohazard Prevention and Geoenvironment Protection, College of Environment and Civil Engineering, Chengdu University of Technology, Chengdu 610059, China
Qiang Luo: School of Civil Engineering, Southwest Jiaotong University, Chengdu 610031, China

for Portland cement [5], which can be produced by the alkalization activation of different industrial by-products or natural mineral admixtures [6–8]. Relevant studies [9] have shown that the CO_2 emitted from geopolymer concrete is around 5–6 times lower than that of ordinary cement concrete. At present, the research and application of geopolymers are mainly based on fly ash (FA) [10,11], and there are few studies on coal gangue (CG)-based geopolymer concrete [12]. Due to the long-term coal mining, a large amount of CG is produced in China, resulting in land occupation and pollution of the atmospheric and water environment [13,14]. Existing studies have shown that calcined CG is rich in amorphous aluminosilicates, which can be used as precursors for preparing geopolymer. However, due to the low calcium content of CG, the compressive strength of CG-based geopolymer concrete is more down than slag-based geopolymer concrete [15]. Researchers usually mix CG and other silica–alumina raw materials to prepare geopolymers. For example, Huang *et al.* [16] prepared geopolymers by mixing calcined CG with blast furnace slag and slaked lime. The results show that the strength of the geopolymer is improved with the increased calcium content.

In addition, the construction industry faces two major issues, excessive consumption of non-renewable resources and the significant accumulation of construction waste. A large amount of natural sand and gravel resources are gradually consumed, leading to a shortage of natural resources. At the same time, due to the "metabolism" of the city itself, a large amount of renovation, demolition, and other activities have led to a large accumulation of construction waste. Therefore, scholars have proposed recycled concrete technology to improve construction waste's resource conversion rate [17,18]. In recent decades, many researchers have thoroughly studied recycled aggregate concrete (RAC) [19–23]. Many experimental results show that recycled aggregate adversely affects the mechanics and durability of concrete, especially when the replacement rate of recycled aggregate exceeds 30% [24]. However, people were pleasantly surprised to find that the performance of recycled aggregate applied to geopolymer is better than that used to cement [25,26], which may be attributed to the higher density of geopolymer matrix compared to ordinary concrete matrix, which can bind more tightly with recycled aggregates [27].

However, low tensile strength and brittle failure are the biggest problems in the application and promotion of GRC [28]. Fiber can significantly improve the tensile strength of GRC, control the development of cracks, and reduce the brittleness of GRC [29–31]. Xu *et al.* [32] found that steel fibers (SFs) can improve the tensile and flexural properties of GRC. When the fiber content was 2.50%, the 28 days compressive strength, tensile strength, and flexural strength were increased by 15.72, 64.10, and 60.95%. In the subsequent study, Xu *et al.* [33] compared the toughening effect of different fibers and analyzed the toughening mechanism of fibers by observing crack growth and scanning electron microscope (SEM). Excessive addition of SF in GRC will reduce its strength. The improved interface strength of SF and GRC can further improve the performance of GRC reinforced by SF. The composite of nanomaterials and SFs is an effective way.

The improvement of compressive strength of GRC reinforced by SF is not obvious, while nanomaterials can make up for this defect [34]. There are many reports on the modification effect of nanomaterials on the interface between fiber and cement [35]. Researchers have found that many nanomaterials such as nano-SiO_2 (NS), nano-Al_2O_3 (NA) [36], graphene oxide [37], and carbon nanofibers [38] can improve the microstructure of the interface between fibers and cement matrix, which greatly improves the performance of the fiber–cement interface strength. However, there are few studies on the influence of nanomaterials on the interfacial strength of fibers and geopolymers. Adak *et al.* [34] found that NS can increase the bond strength between steel bars and geopolymer concrete by 28.78% through pull-out tests, but the enhancement mechanism was not discussed. Alomayri [39] studied the effect of nano-$CaCO_3$ (NC) on the properties of basalt fiber geopolymer concrete and found that NC improved the compressive, flexural, and impact strength of basalt geopolymer concrete. This can be attributed to the promotion of geopolymerization reaction and the enhancement of ITZ by NC. This research shows in detail that nanomaterials are also beneficial to the interfacial strength of geopolymers and basalt fiber. However, to the best of my knowledge, the effects of NA particles on the microstructures and mechanical properties of CG-based geopolymer have not yet been reported. NA particles can dissolve in an alkaline activator solution, which may increase the amount of geopolymer gel formed and the interfacial strength of geopolymers and SF. This research will encourage the usage of NA and SF for developing a good geopolymer composite paste in construction applications.

In summary, CG-based geopolymer recycled concrete is a promising green building material that can not only solve the treatment problems of waste concrete and CG solid waste but also reduce the mining of natural stone, the use of cement, and the emission of atmospheric pollutants. It has significant environmental, economic, and social benefits. Currently, more research has focused on improving the concrete performance of single-doped fibers or nanomaterials, but these two methods still have certain limitations. At the same time, summarizing the research status, we found that the two can complement each other in terms of

modification effects, but few studies have combined the two. Based on this, it is necessary to explore the synergistic modification effect and mechanism of nanomaterials and fibers on CG-based geopolymer recycled concrete.

In this article, the effects of SF and NA on the mechanical properties and micromorphology of GRC were studied. First, GRC was prepared by using calcined CG, FA, slag, and recycled aggregate. On this basis, the effects of SF and NA content on the mechanical properties of GRC were studied, and the micromorphology of GRC was analyzed by SEM. The purpose is to explore the engineering performance and application potential of the GRC reinforced by SF and NA and to provide research cases and data support.

2 Materials and methods

2.1 Experimental materials

The calcined CG, low-calcium FA, and blast-furnace slag used in this study were produced by Huashuo Mineral Powder Factory, Lingshou County, Hebei Province. The chemical composition reported by the producer is reported in Table 1. Their morphologies are shown in Figure 1(a)–(c).

The alkaline activators used in this study were sodium silicate (Na_2SiO_3) and sodium hydroxide (NaOH), as shown in Figure 1(d) and (e). The appearance of sodium silicate is a translucent viscous liquid, the modulus is 2.2, and the moisture content is 65%. Sodium hydroxide is produced by Jinan Chuanfeng Trading Co., Ltd. It is a sheet solid with a purity of 99%, a melting point of 378°C, and a boiling point of 1,344°C.

The fine aggregate obtained from a local supplier has been used in this study, with an apparent density of 2,600 kg·m^{-3}, a bulk density of 1,550 kg·m^{-3}, a fineness modulus of 2.52, and a moisture content of 2.3%. The coarse aggregate is commercially available continuously graded pebbles with a particle size of 5–20 mm, an apparent density of 2,745 kg·m^{-3}, a bulk density of 1,460 kg·m^{-3}, and a mud content of 0.1%.

The recycled coarse aggregate used in this study was produced by Luosong's new building materials factory in Chengdu, Sichuan Province. After the screening, it was made into 5–20 mm continuously graded aggregate, as shown in Figure 1(f). The apparent density is 2,403 kg·m^{-3}, the stacking density is 1,380 kg·m^{-3}, the mud content is 0.67%, the water absorption is 4.6%, and the crushing value is 14.37%.

Corrugated SF was used in this study which was produced by Hebei Demai Wire Mesh Products Co., Ltd., and its performance index is shown in Table 2. The physical photograph is shown in Figure 1(g).

Nano-Al_2O_3 used in this study was produced by Taipeng New Materials Co., Ltd, and relevant technical parameters are shown in Table 3. The physical photograph is shown in Figure 1(h).

2.2 Mix proportion design

Based on the preliminary orthogonal experiments, the CG:FA:slag ratio was determined as 2:1:1, the aggregate cement material ratio was 4.0 (the replacement rate of recycled aggregate was 40%), the sand ratio was 0.39, the water–binder ratio was 0.4, and the alkali activator modulus was 1.5 to prepare CG-based geopolymer concrete specimens. On this basis, the effects of SF with different content (volume fraction ranged from 0.25 to 1.25%) on the properties of the geopolymer concrete were investigated. The mix proportion is shown in Table 4.

2.3 Specimen preparation and curing

The procedure of specimen preparation is shown in Figures 2 and 3, and the detailed steps are as follows:

1) The alkali activator was prepared before use and cooled at room temperature for 12 h.
2) The silica–alumina powder materials were put into the agitator, stirred for 1 min until mixed evenly; then alkali excitation solution was added and stirred for 2 min.
3) The sand, natural coarse aggregate and recycled coarse aggregate were added and mixed evenly again for 6 min.
4) The concrete mixture was put into the corresponding mold and vibrated to dense.

Table 1: Chemical composition of cementitious materials

Materials	SiO_2 (%)	Al_2O_3 (%)	Fe_2O_3 (%)	CaO (%)	MgO (%)	MnO (%)	H_2O (%)	S (%)	pH	Burn vector (%)
CG	52	45	40.30	≤0.5	0.26		≤0.3	0.24	6.5–6.8	
Slag	37.2	13.6	5	32.55	4.5	1.5			6.33	3
FA	52.5	19.6	5.21	4	1.45			0.24		≤5

Figure 1: Experimental materials: (a) CG, (b) FA, (c) slag, (d) sodium silicate, (e) NaOH, (f) RCA, (g) SF, and (h) NA.

Table 2: Performance parameters of SF

Performance	Length (mm)	Diameter (mm)	Density ($g \cdot cm^{-3}$)	Tensile property (MPa)
Parameter	35	2	7.85	577

Table 3: Performance parameters of nano-Al_2O_3

Performance	Specific surface area ($m^2 \cdot g^{-1}$)	Particle size (nm)	Bulk density ($g \cdot L^{-1}$)	Purity (wt%)	pH
Parameter	22–50	20	0.2–0.4	96	6–9

Table 4: SFGRC mix proportion (kg·m^{-3})

Mix no.	CG	FA	Slag	Sodium silicate	NaOH	Sand	Recycled/natural coarse aggregate	SF
GRC	211.9	105.95	105.95	262.76	18.22	661.13	517.04/517.04	0
SF-0.25	211.9	105.95	105.95	262.76	18.22	661.13	517.04/517.05	19.63
SF-0.5	211.9	105.95	105.95	262.76	18.22	661.13	517.04/517.06	39.25
SF-0.75	211.9	105.95	105.95	262.76	18.22	661.13	517.04/517.07	58.88
SF-1.0	211.9	105.95	105.95	262.76	18.22	661.13	517.04/517.08	78.5
SF-1.25	211.9	105.95	105.95	262.76	18.22	661.13	517.04/517.09	117.75

5) The specimen was coated with lubricating oil and placed in a drying chamber at 20°C for 24 h.
6) The specimen was taken out of the mold, the surface of the test block was wrapped with plastic film and sealed, and then put into an oven at 100°C for curing for 12 h. After high-temperature curing, the test block shall be placed in the room at about 20°C to continue curing until the specified time (7 and 28 days).

2.4 Experiment apparatus and test methods

The mechanical properties of concrete were tested per "Standard for Test Methods of Fiber Reinforced Concrete (CECS13-2009)" and "Standard for Test Methods of Physical and Mechanical Properties of Concrete (GB/T50081-2019)." The main test apparatus and equipment used in this study are shown in Figure 4.

2.4.1 Compressive strength test

The specimen's size used for compressive strength test is 100 mm × 100 mm × 100 mm. The side of the specimen is placed in the center area of the pressure plate for compression testing. The loading speed is set at 0.5 MPa·s^{-1}. In order to reduce the error, each group is set with three specimens, and the compressive strength is taken from the arithmetic average of the three specimens. The compressive strength is calculated by the following formula:

$$f_{cu} = 0.95\frac{F}{A}, \tag{1}$$

where F is the compressive failure load (N) and A is the bearing area of the specimen (mm^2).

2.4.2 Splitting tensile strength test

The specimens for the splitting tensile strength test are 100 mm × 100 mm × 100 mm. The specimen is placed in the splitting tensile test fixture and placed in the central area of the pressure plate. Then the strip pads are placed between the bearing plate and the specimen, and their positions are adjusted to ensure the alignment of the specimen with the strip pads. Finally, the specimen is loaded at a uniform rate of 0.05 MPa·s^{-1}. Similarly, a strength test of three identical specimens is carried out for each group,

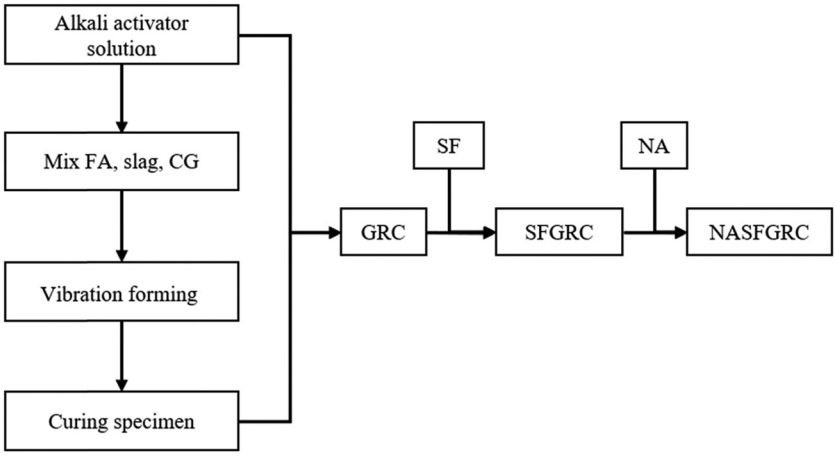

Figure 2: Production flow chart.

Figure 3: Sample preparation and curing: (a) pouring and vibrating, (b) solidification, (c) demolding, and (d) high-temperature curing.

Figure 4: Laboratory apparatus. (a) Machine for compressive test, (b) machine for splitting tensile test, (c) machine for flexural test, and (d) SEM.

and then the tensile strengths are averaged as the final strength. The splitting tensile strength is calculated according to the following formula:

$$f_{ts} = \frac{2F}{\pi A} = 0.637 \times \frac{F}{A}, \quad (2)$$

where F is the splitting failure load (N) and A is the bearing area of the splitting (mm^2).

2.4.3 Flexural strength test

The specimens for the flexural strength test are 100 mm × 100 mm × 400 mm. To ensure the accuracy of the data, we adjusted the first test apparatus of the steel loading to the appropriate position to 0.05 MPa·s^{-1} loading speed uniform loading until the test block was damaged. Similarly, a strength test of three identical specimens is carried out for each group, and then the flexural strengths are averaged as the final strength. The flexural strength is calculated according to the following formula:

$$f_{cc} = 0.85 \times \frac{Fl}{bh^2}, \quad (3)$$

where F is the flexural failure load (N), A is the bearing area of the splitting (mm^2), and b and h are the section width and height of the specimen, respectively (mm).

2.4.4 Micromorphology analysis

The equipment model used for the test was a Prisma E SEM from Thermo Fisher Scientific. After the splitting tensile test, the fragments containing fibers are selected. The fragments were soaked in anhydrous ethanol for 3 h, stopped hydration, and then put them into an oven to dry for 24 h. These were sealed and stored in a transparent plastic bag to prevent the sample surface from being stained before it was scanned with an SEM.

3 Research results and discussion

3.1 Influence of SF dosages on the strength of SFGRC

3.1.1 Compressive strength

The morphology of GRC and SFGRC after failure is shown in Figure 5. There is an obvious sound when GRC is destroyed. As shown in the red line, there are many cracks and fragments on the surface of GRC, showing obvious brittle failure. On the contrary, there are few fragments when SFGRC is destroyed.

It can be seen from Figure 6 that the 7 and 28 days compressive strengths of the reference group without SF are 28.14 and 33.88 MPa, respectively. When the SF content was 0.25, 0.5, and 0.75%, the 7 days compressive strength of SFGRC was 29.49, 31.44, and 29.75 MPa, and the strength growth rates were 4.8, 11.73, and 5.72%, respectively. The 28 days compressive strength was 35.92, 37.6, and 34.73 MPa, respectively, and the growth rates of 28 days were 6.02, 10.98, and 2.51%, respectively. According to the compressive strength data of 7 and 28 days, the optimum content of SF is 0.5%. There was tensile stress concentration in the internal micropores and microcracks, resulting in the formation of cracks parallel to the load direction. The addition of fibers can make the expansion path of the crack tip be forced to change the extension direction or cross the fiber to form a finer crack field after encountering the fiber, thereby increasing the energy consumed by the crack development and slowing the

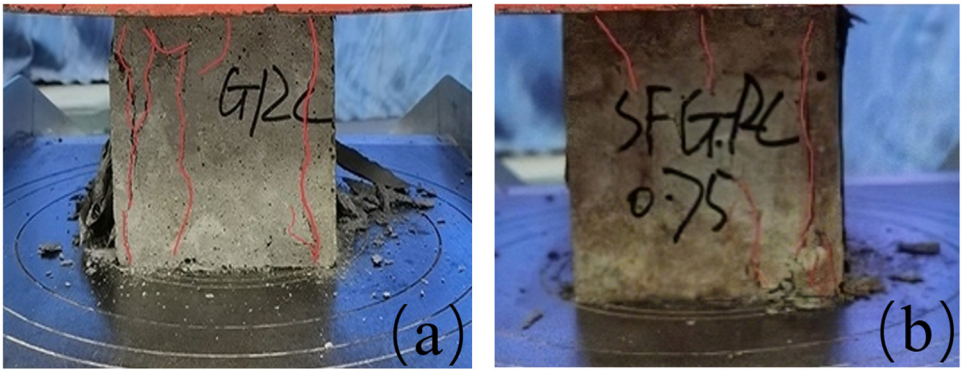

Figure 5: Compressive failure morphology: (a) GRC and (b) SFGRC.

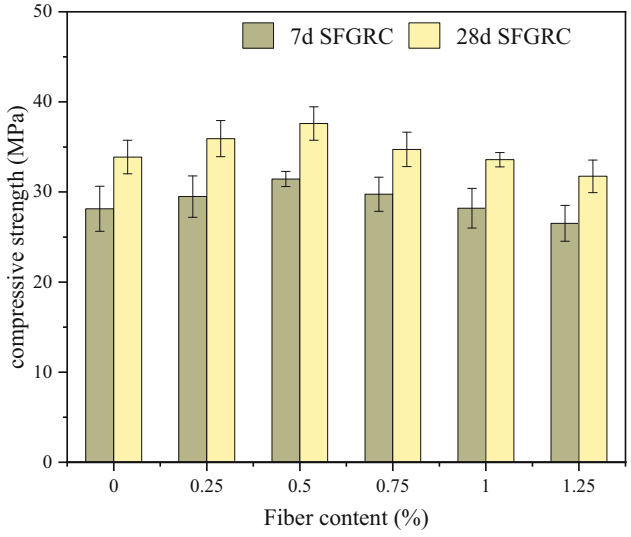

Figure 6: Compressive strength.

expansion of the crack. Therefore, the compressive strength of SFGRC is improved [40]. When the content of SF reaches 1%, the growth rate of compressive strength is almost zero, while when the content of SF is 1.25%, the compressive strength of 7 and 28 days decreases by 5.76 and 6.32%. The compressive strength of SFGRC showed a downward trend after increasing the SF content to 1.0%. This phenomenon may be due to two reasons: (i) when the SF content is too high, it does not distribute well in the matrix and leads to the "agglomeration" phenomenon, which introduces more micropores in the structure and reduces its improving effect on the concrete or even causes negative effects; (ii) due to the volume limitation of the concrete specimen itself, excessive SF admixture can produce serious boundary effects, *i.e.*, there may be too many SFs at a certain location, causing a decrease in concrete strength [41].

3.1.2 Splitting tensile strength

The split failure morphology is shown in Figure 7. GRC was split into two along a straight crack with a loud sound, which was a brittle failure. After incorporating SF, SFGRC showed the phenomenon of cracking but not breaking, which was a ductile failure.

Figure 8 shows the splitting tensile strength of SFGRC. The 7 and 28 days split tensile strengths of GRC were 1.85 and 2.17 MPa, respectively. When the SF content was 0.25, 0.5, and 0.75%, the splitting tensile strength of SFGRC was 2.35, 2.73, and 3.05 MPa in 7 days, and 2.58, 2.89, and 3.38 MPa in 28 days, respectively. The growth rate of splitting tensile strength of SFGRC was 27.03, 47.57, and 64.86% in 7 days and 18.89, 33.18, and 55.76% in 28 days, respectively. The tensile strength in concrete mainly depends on

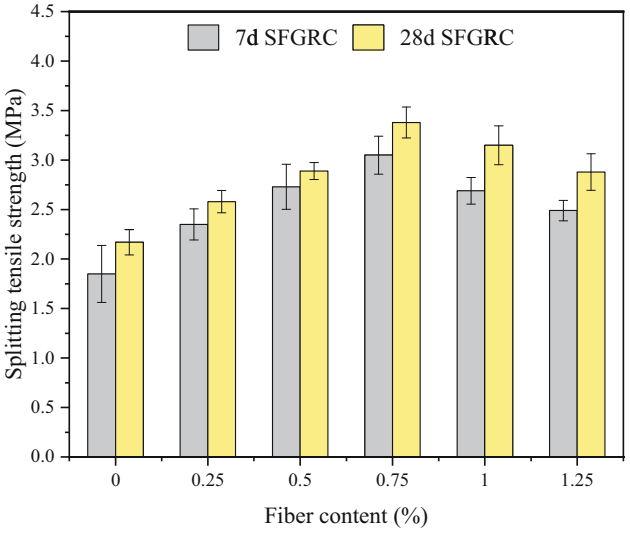

Figure 8: Splitting tensile strength.

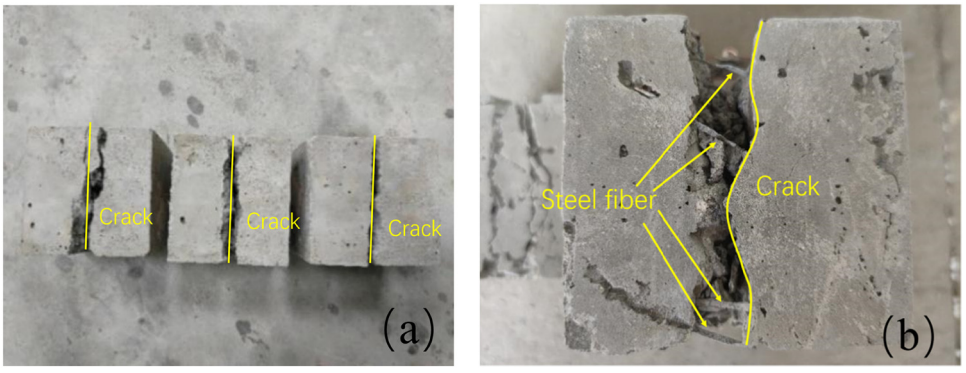

Figure 7: Morphology of splitting tensile failure: (a) GRC and (b) SFGRC.

the bond strength between the aggregate and the matrix, while the tensile strength of concrete after adding SF depends on the bond strength between the SF and the matrix. The fibers spanning the cracks bear part of the tensile stress, which alleviates the stress concentration at the crack tip, effectively constrains the expansion of the cracks, and thus improves the splitting tensile strength of GRC. When the content of SF exceeded 0.75%, the growth rate of splitting tensile strength of SFGRC declined. The reason is that the SF cannot play a bridging role effectively due to its agglomeration [41].

3.1.3 Flexural strength

The failure mode of GRC is shown in Figure 9. The crack developed from the bottom of the specimen and quickly penetrated the section. The fracture surface was relatively smooth, and the aggregate was pulled off, showing obvious brittle failure. SFGRC was a ductile failure, and the specimen did not break into two halves. As shown by the red line in Figure 9, the crack was generated from the bottom of the sample and developed slowly upward, showing a zigzag shape. The SF spans both ends of the crack and bears the tensile stress, so the flexural strength and ductility were improved. After the failure, it can continue to bear the load until the specimen is completely broken.

Figure 10 shows the 7 and 28 days flexural strength of GRC were 4.16 and 4.59 MPa, respectively. SF could significantly improve the flexural strength of GRC, which is consistent with splitting tensile strength. When the SF content was 0.25, 0.5, and 0.75%, the splitting tensile strength of SFGRC was 4.52, 4.93, and 5.27 MPa in 7 days and 4.93, 5.2 and 5.57 MPa in 28 days. The growth rate of splitting tensile strength of SFGRC was 8.65, 18.51, and 26.68% in 7 days and 7.41, 13.29, and 21.35% in 28 days. The randomly distributed SF not only hindered crack development but also restricted the direction of crack development to a certain extent. At the same time, SF reduced the stress concentration at the crack tip, bridged the voids and cracks in the matrix, improved the bending strength of SFGRC, and achieved the purpose of improving the strength and crack resistance of GRC.

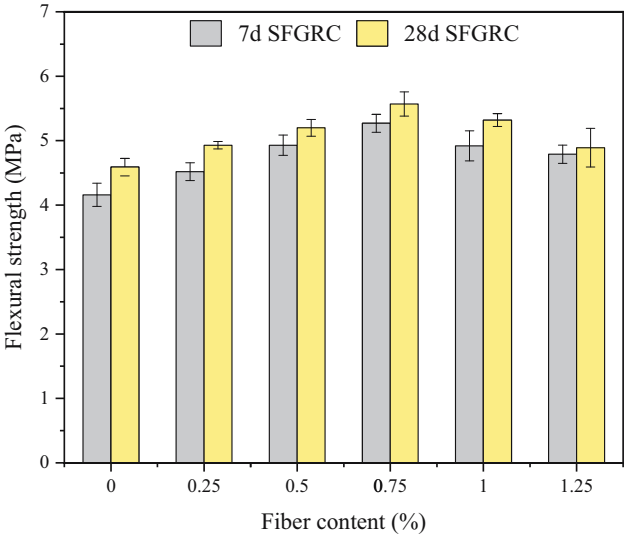

Figure 10: Flexural strength.

3.2 Influence of NA dosages on the strength of SFGRC

According to the mechanical property test results of SFGRC, the best SF content (0.75%) was selected as the control

(a) GRC (b) SFGRC

Figure 9: Morphology of flexural failure: (a) GRC and (b) SFGRC.

group to explore the modification effect of different NA content (0, 0.5, 1, 1.5, and 2%).

3.2.1 Compressive strength

The compressive strength of NASFGRC test results is shown in Figure 11. NA significantly improved the compressive strength of NASFGRC. The reference group compressive strength of SFGRC was 31.44 MPa in 7 days and 37.6 MPa in 28 days, respectively. When the NA content was 1.5%, the compressive strength of NASFGRC reached the maximum of 39.09 MPa in 7 days and 45.71 MPa in 28 days. The improvement rate of compressive strength was 24.33 and 21.57%, respectively, similar to the experimental results of Dişçi and Polat [42]. The enhanced compressive strength of the geopolymer nanocomposites is due to the improvement in pore-filling mechanisms. When NA is uniformly dispersed, it fills voids in the matrix, creating a denser microstructure [43]. According to the experimental data, the compressive strength at 7 days increases faster, which indicates that NA particles promote the process of early hydration polymerization. The data at 7 and 28 days indicate that the optimal content of NA is 1.5%. When the content of NA exceeds 1.5%, the compressive strength growth rate of NASFGRC showed a downward trend, which illustrates that the continued addition of excessive NA has a negative impact on the strength of NASFGRC. The presence of NA content threshold may be due to the excessive number of NA particles and the excessive van der Waals forces between them, leading to the aggregation effect. The aggregated particles in the geopolymer matrix cannot promote the reaction of geopolymer but also lead to the formation of micropores, which are not conducive to the strength of the material in essence.

3.2.2 Splitting tensile strength

The split tensile strength of the NASFGRC test result is shown in Figure 12. The tensile strengths of the reference group 7 and 28 days are 3.05 and 3.38 MPa, respectively. When the NA content was 1%, the split tensile strength of NASFGRC reached the maximum of 3.47 MPa in 7 days and 3.87 MPa in 28 days. The increase rate of tensile strength of NASFGRC was 13.77 and 14.5%, respectively.

This enhancement of the bending capacity of geopolymer nanocomposites and the overcoming of local failures can be attributed to good interfacial adhesion leading to superior resistance to bending and fracture forces. NA particles bridge the microcracks and enhance the crack growth resistance, which leads to an increase in splitting tensile strength. In addition, NA enhanced the interface bond strength between the SF and the geopolymer [36]. The uniformly dispersed NA affected the geopolymer reaction and promoted an Al-rich gel formation, which filled the pore and increased the density of the microstructure in the interface between the SF and the geopolymer. When the content of NA exceeds 1.0%, the increase in the split tensile strength of the material shows a downward trend. When the NA content was 2%, the split tensile strength of NASFGRC was 3.14 MPa in 7 days and 3.52 MPa in 28 days. This may be because of agglomerations of NA in the geopolymer matrix creating micro-void stress concentrators, which are essentially weak zones in the material.

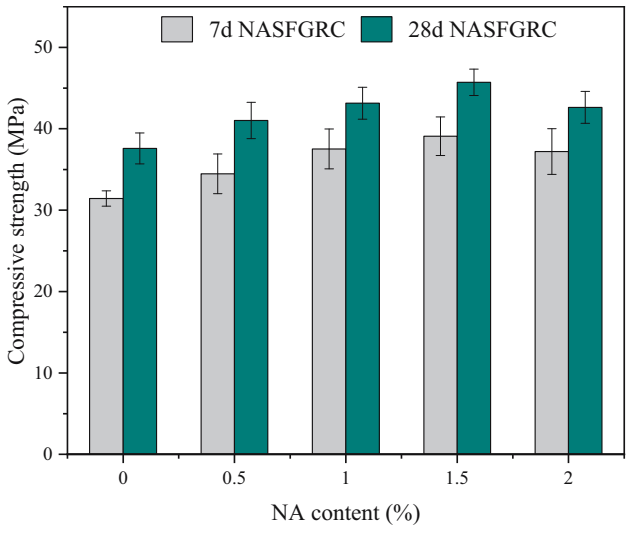

Figure 11: Compressive strength of NASFGRC.

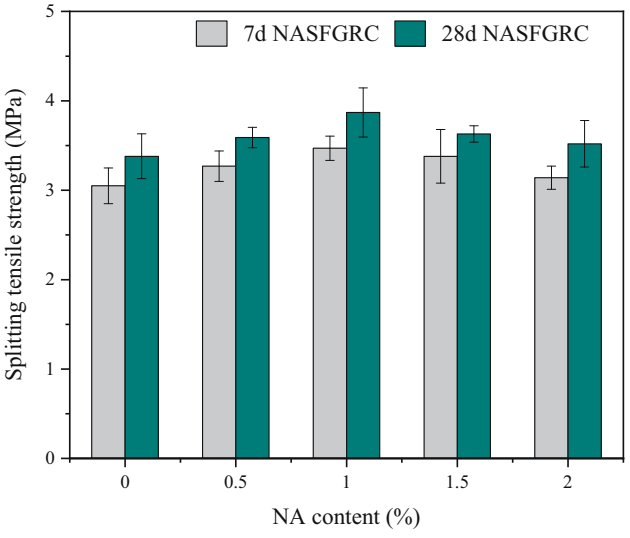

Figure 12: Splitting tensile strength of NASFGRC.

3.2.3 Flexural strength

The flexural strength of NASFGRC at different ages is shown in Figure 13. The 7 and 28 days strength of the reference group are 5.27 and 5.57 MPa, respectively. When the NA content was 1%, the flexural strength of NASFGRC reached the maximum of 5.69 MPa in 7 days and 6.02 MPa in 28 days. The increase rate of tensile strength of NASFGRC was 7.97 and 8.08%, respectively. When the content of NA exceeds 1%, its strength begins to decline. This is also because the huge specific surface area of excessive NA is easy to agglomerate in the matrix, and part of the free water of the hydration reaction is wrapped by NA, which hinders the hydration reaction and increases the micropores in NASFGRC. Different from the compressive strength and the splitting tensile strength, NA is not obvious for improving the flexural strength of concrete, because the flexural strength mainly depends on the anchoring force of the fiber.

3.3 Micromorphology analysis

3.3.1 Micromorphology of geopolymer matrix

Figure 14 shows the SEM images with a magnification of 3,000–10,000 times the 28 days geopolymer matrix, which will show the influence of NA on the microstructure and hydration products. In the reference group, there were many holes and cracks in the matrix, the micromorphology was relatively loose, and the distribution of hydration products was uneven. The microstructure is enhanced with the improvement of NA incorporation. NA-0.5 (Figure 14(b)) has a relatively small number of pores in the matrix during the hydration products increase. The density of the matrix is slightly better than that of the reference sample, but an incomplete reaction of FA particles and microcracks can be observed. It can be seen in NA-1.0 (Figure 14(c)) that some microcracks have disappeared, NA has greatly promoted the polymerization reaction, and a large number of hydration products have formed a compact structure. NA-1.5 (Figure 14(d)) shows that the silicon aluminum material is more thoroughly reflected, the microstructure is denser, and microcracks can hardly be seen. Figure 14(e) shows two kinds of gels with different structures, the layered C–A–S–H gel and the spongy N–A–S–H gel, which are the main source of the strength of the geopolymer. The improvement of NASFGRC microstructure can be attributed to the nucleation effect and filling effect. The nucleation effect imports hydration speed and the creation of hydrated products, reducing the size and number of unreacted FA particles. The filling effect is that NA with a nanometer scale filled the pore in the N(C)–A–S–H gel, which improves the elastic modulus tested by nanoindentation [44].

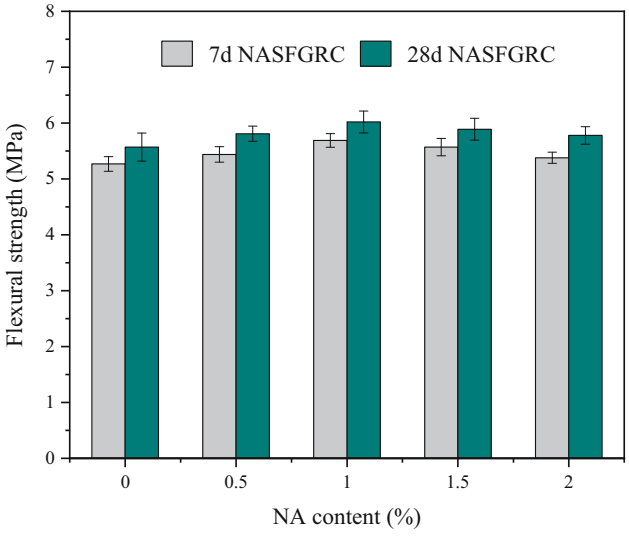

Figure 13: Flexural strength of NASFGRC.

3.3.2 Micromorphology of the interface between SF and matrix

The interface bonding between SF and the matrix is shown in Figure 15(a). SF is closely embedded in the geopolymer matrix. When the GRC is subjected to external force, SF can bear part of the stress, which is the positive effect of SF. Therefore, the 28 days splitting tensile strength and flexural strength of SFGRC with different SF content increased by 18–55.76 and 7–21.35%, respectively. There are a certain number of additional holes on the interface and matrix caused by SF, which is a negative effect of SF incorporation. The proper amount of SF can improve the mechanical properties because the positive effect is greater than the negative effect. Excess amounts of SF will lead to the increase of pores, and the SF will also agglomerate, as shown in Figure 15(b), so the mechanical properties of GRC gradually decline.

The microstructure of the interface between SF and the matrix is shown in Figure 16(a). It is observed that there is a crack between the SF and the geopolymer matrix, and the hydration products are relatively loose. There are a lot of calcium hydroxide crystals (CH), which may be caused by the reaction between the old mortar adhered to the recycled aggregate and the geopolymer. A higher proportion of CH will greatly reduce the strength of the

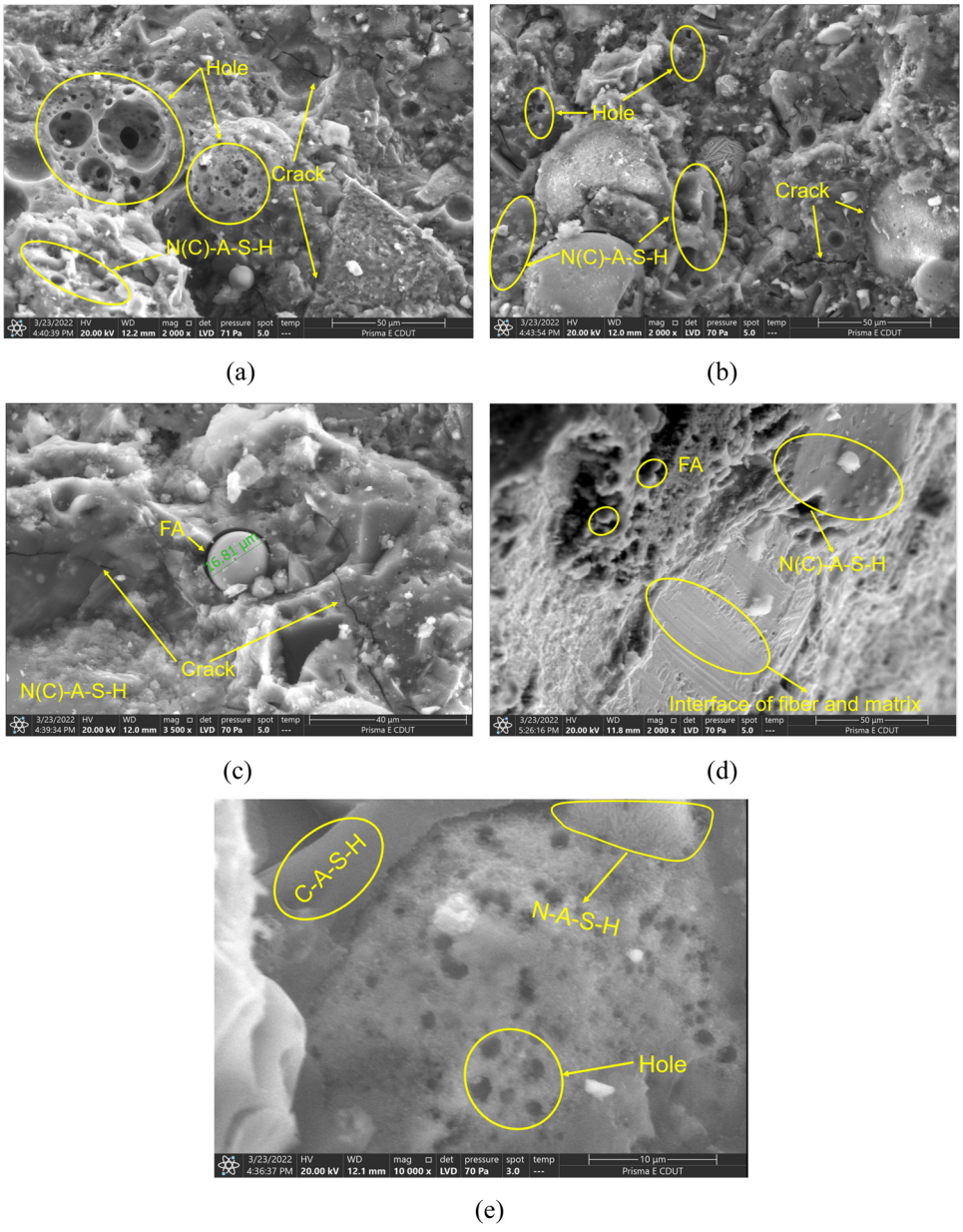

Figure 14: Micromorphology of geopolymer matrix. (a) NA-0, (b) NA-0.5, (c) NA-1.0, (d) NA-1.5, and (e) NA-2.0.

interface transition zone [45]. It can be seen in NASFGRC-0.5 (Figure 16(b)) and NASFGRC-1.0 (Figure 16(c)) that the hydration products increase significantly. It may be seen that the NA act as the crystal nucleus of the hydration products to the formation of extra C(N)–A–S–H gels in the geopolymer matrix [46]. At the same time, the crack width between the SF and the matrix decreases significantly. In NASFGRC-1.5 (Figure 16(d)), there are almost no unreacted FA particles, and the crack between SF and the matrix is closer. Therefore, the compressive strength, splitting tensile strength, and flexural strength of NASFGRC are increased by 21.57, 7.4, and 5.75%, respectively. The hydration products of NASFGRC-2.0 (Figure 16(e)) are relatively dense whole, but microcracks increase, which may be caused by the agglomeration of NA, which corresponds to the mechanical property test results. Excessive content will lead to NA agglomeration, which will make the excellent performance of nanoparticles cannot be fully exerted and will affect the macroperformance of concrete.

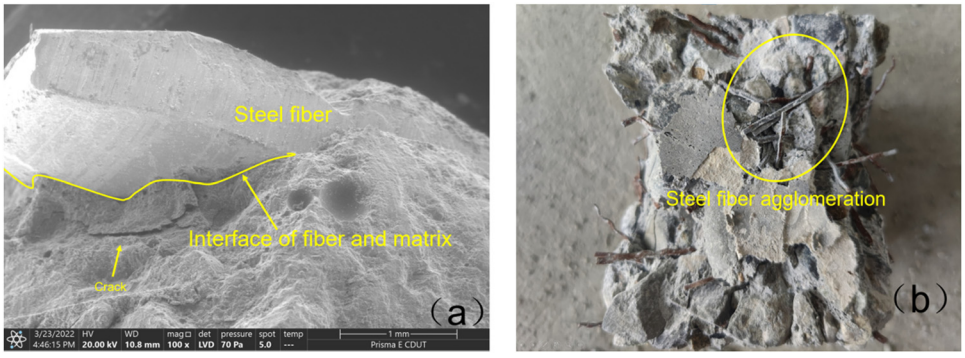

Figure 15: (a) Interface between SF and matrix and (b) SF agglomeration.

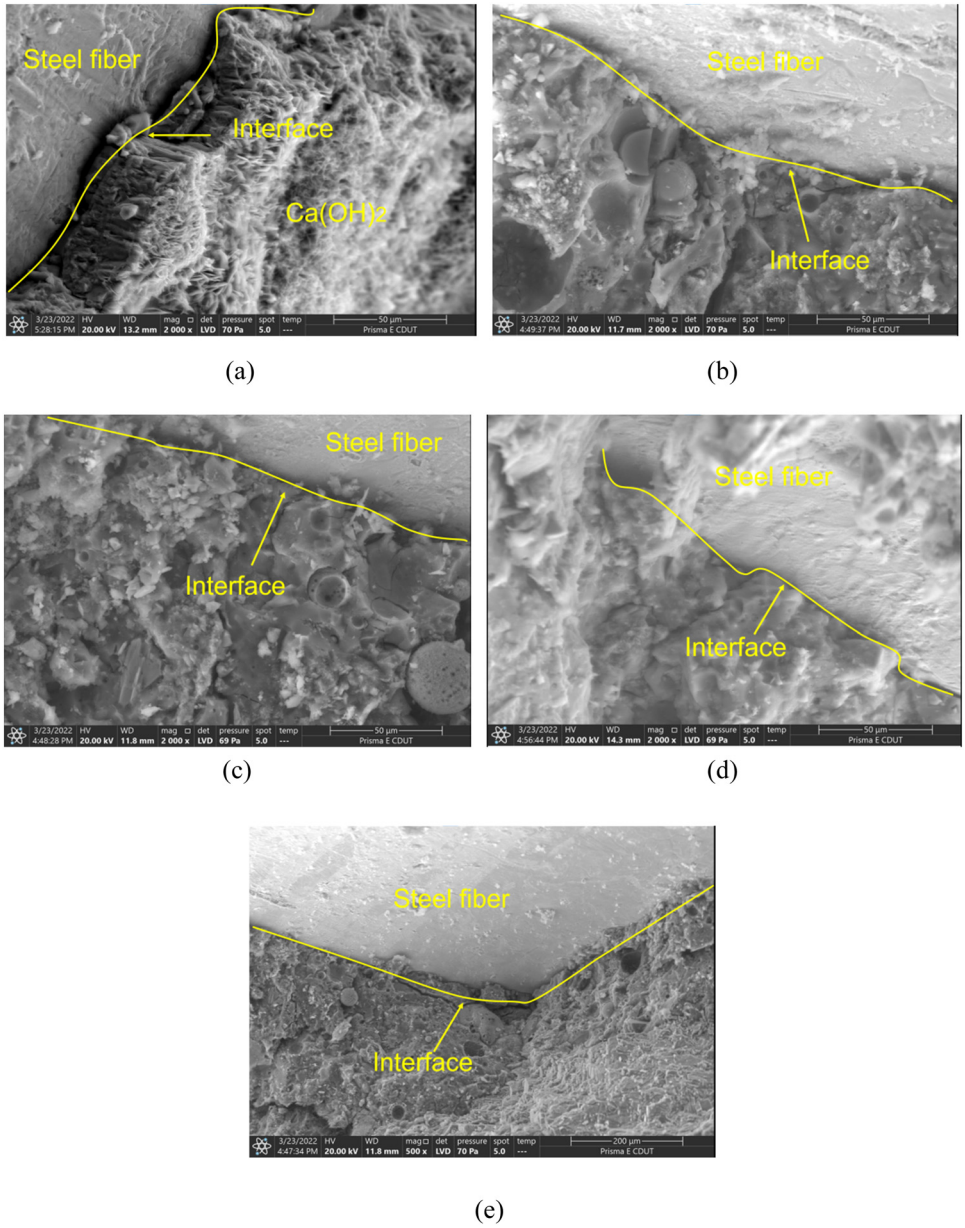

Figure 16: Micromorphology of the interface. (a) SFGRC, (b) NASFGRC-0.5, (c) NASFGRC-1.0, (d) NASFGRC-1.5, and (e) NASFGRC-2.0.

4 Conclusion

This study focuses on CG-based geopolymer recycled concrete and investigates the effects of single addition of SF and SF-NA synergy on its mechanical properties and microstructure. The following conclusions were obtained:

1) SF can significantly improve the tensile and flexural strength of concrete, but it cannot significantly improve the compressive strength of concrete.
2) The addition of NA can obviously improve the compressive strength of SFGRC and further improve the tensile and flexural strength of SFGRC.
3) NA not only improves the microstructure of GRC matrix, making it denser, but also strengthens the bonding between SF and matrix.
4) Excessive SF and NA are unfavorable to the mechanical properties of GRC, because too much doping will lead to agglomeration, which is detrimental to property development. Therefore, the appropriate doping amount should be selected during the preparation process.

Acknowledgments: The writing of this article has been supported by many projects, which can be seen in funding information. At the same time, the project team members and all authors have supported this article, a note of thanks to them. The authors thank the State Key Laboratory of Geohazard Prevention and Geoenvironment Protection (Chengdu University of Technology) for providing the working environment and scientific research conditions for their scientific research team.

Funding information: This study was supported by the Higher Education Personnel Training Quality and Teaching Reform Project of Sichuan Province (JG2021-730), Philosophy and Social Science Research Fund Project of Chengdu University of Technology (YJ2022-ZD015), Open research project of Meteorological Disaster Prediction, Warning and Emergency Management Research Center (ZHYJ22-YB02), Development Funding Program for Young and Middle-aged Key Teachers of Chengdu University of Technology (10912-JXGG2021-01003), Sichuan Ming yang Construction Engineering Management Co., Ltd. Specialized Project (MY2021-001), and College Students' Innovation and Entrepreneurship Training Program (S202210616013, S202210616015).

Author contributions: All authors have accepted responsibility for the entire content of this manuscript and approved its submission.

Conflict of interest: The authors state no conflict of interest.

Data availability statement: The data that support the findings of this study are available from the corresponding author upon reasonable request.

References

[1] Amran, Y. H. M., R. Alyousef, H. Alabduljabbar, and M. El-Zeadani. Clean production and properties of geopolymer concrete; A review. *Journal of Cleaner Production*, Vol. 251, 2020, id. 119679.
[2] Davidovits, J. Geopolymers and geopolymeric materials. *Journal of thermal analysis*, Vol. 35, 1989, pp. 429–441.
[3] Fahim Huseien, G., J. Mirza, M. Ismail, S. K. Ghoshal, and A. Abdulameer Hussein. Geopolymer mortars as sustainable repair material: A comprehensive review. *Renewable and Sustainable Energy Reviews*, Vol. 80, 2017, pp. 54–74.
[4] Ren, B., Y. Zhao, H. Bai, S. Kang, T. Zhang, and S. Song. Eco-friendly geopolymer prepared from solid wastes: A critical review. *Chemosphere*, Vol. 267, 2021, id. 128900.
[5] Chen, K., D. Wu, L. Xia, Q. Cai, and Z. Zhang. Geopolymer concrete durability subjected to aggressive environments – A review of influence factors and comparison with ordinary Portland cement. *Construction and Building Materials*, Vol. 279, 2021, id. 122496.
[6] Shilar, F. A., S. V. Ganachari, V. B. Patil, T. M. Y. Khan, S. Javed, and R. U. Baig. Optimization of alkaline activator on the strength properties of geopolymer concrete. *Polymers*, Vol. 14, 2022, id. 2434.
[7] Jindal, B. B., T. Alomayri, A. Hasan, and C. R. Kaze. Geopolymer concrete with metakaolin for sustainability: A comprehensive review on raw material's properties, synthesis, performance, and potential application. *Environmental Science and Pollution Research*, Vol. 30, 2023, pp. 25299–25324.
[8] Nagajothi, S., S. Elavenil, S. Angalaeswari, L. Natrayan, and W. D. Mammo. Durability studies on fly ash based geopolymer concrete incorporated with slag and alkali solutions. *Advances in Civil Engineering*, Vol. 2022, 2022, id. 7196446.
[9] Rabiaa, E., R. A. S. Mohamed, W. H. Sofi, and T. A. Tawfik. Developing geopolymer concrete properties by using nanomaterials and steel fibers. *Advances in Materials Science and Engineering*, Vol. 2020, 2020, id. 5186091.
[10] Their, J. M. and M. Özakça. Developing geopolymer concrete by using cold-bonded fly ash aggregate, nano-silica, and steel fiber. *Construction and Building Materials*, Vol. 180, 2018, pp. 12–22.
[11] Biondi, L., M. Perry, C. Vlachakis, Z. Wu, A. Hamilton, and J. McAlorum. Ambient cured fly ash geopolymer coatings for concrete. *Materials*, Vol. 12, 2019, id. 923.
[12] Zhang, W., C. Dong, P. Huang, Q. Sun, M. Li, and J. Chai. Experimental study on the characteristics of activated coal gangue and coal gangue-based geopolymer. *Energies*, Vol. 13, 2020, id. 2504.
[13] Song, L., S. Liu, and W. Li. Quantitative inversion of fixed carbon content in coal gangue by thermal infrared spectral data. *Energies*, Vol. 12, 2019, id. 1659.

[14] Huang, Y., J. Zhang, W. Yin, and Q. Sun. Analysis of overlying strata movement and behaviors in caving and solid backfilling mixed coal mining. *Energies*, Vol. 10, 2017, id. 1057.
[15] Moghadam, M. J., R. Ajalloeian, and A. Hajiannia. Preparation and application of alkali-activated materials based on waste glass and coal gangue: A review. *Construction and Building Materials*, Vol. 221, 2019, pp. 84–98.
[16] Huang, G., Y. Ji, J. Li, Z. Hou, and Z. Dong. Improving strength of calcinated coal gangue geopolymer mortars via increasing calcium content. *Construction and Building Materials*, Vol. 166, 2018, pp. 760–768.
[17] Tam, V. W. Y., M. Soomro, and A. C. J. Evangelista. A review of recycled aggregate in concrete applications (2000–2017). *Construction and Building Materials*, Vol. 172, 2018, pp. 272–292.
[18] Silva, R. V., J. de Brito, and R. K. Dhir. Fresh-state performance of recycled aggregate concrete: A review. *Construction and Building Materials*, Vol. 178, 2018, pp. 19–31.
[19] Kim, J. Influence of quality of recycled aggregates on the mechanical properties of recycled aggregate concretes: An overview. *Construction and Building Materials*, Vol. 328, 2022, id. 127071.
[20] Liang, C., H. Ma, Y. Pan, Z. Ma, Z. Duan, and Z. He. Chloride permeability and the caused steel corrosion in the concrete with carbonated recycled aggregate. *Construction and Building Materials*, Vol. 218, 2019, pp. 506–518.
[21] Jang, H., J. Kim, and A. Sicakova. Effect of aggregate size on recycled aggregate concrete under equivalent mortar volume mix design. *Applied Sciences*, Vol. 11, 2021, id. 11274.
[22] Liu, B., C. Feng, and Z. Deng. Shear behavior of three types of recycled aggregate concrete. *Construction and Building Materials*, Vol. 217, 2019, pp. 557–572.
[23] Liu, G., Q. Li, J. Song, L. Wang, H. Liu, Y. Guo, et al. Quantitative analysis of surface attached mortar for recycled coarse aggregate. *Materials (Basel)*, Vol. 15, 2021 , id. 257.
[24] Xiao, J., W. Li, Y. Fan, and X. Huang. An overview of study on recycled aggregate concrete in China (1996–2011). *Construction and Building Materials*, Vol. 31, 2012, pp. 364–383.
[25] Shi, X. S., F. G. Collins, X. L. Zhao, and Q. Y. Wang. Mechanical properties and microstructure analysis of fly ash geopolymeric recycled concrete. *Journal of Hazardous Materials*, Vol. 237–238, 2012, pp. 20–29.
[26] Ren, X. and L. Zhang. Experimental study of interfacial transition zones between geopolymer binder and recycled aggregate. *Construction and Building Materials*, Vol. 167, 2018, pp. 749–756.
[27] Liu, C., X. Deng, J. Liu, and D. Hui. Mechanical properties and microstructures of hypergolic and calcined coal gangue based geopolymer recycled concrete. *Construction and Building Materials*, Vol. 221, 2019, pp. 691–708.
[28] Ranjbar, N. and M. Zhang. Fiber-reinforced geopolymer composites: A review. *Cement and Concrete Composites*, Vol. 107, 2020, id. 103498.
[29] Zheng, Y., J. Zhuo, and P. Zhang. A review on durability of nano-SiO2 and basalt fiber modified recycled aggregate concrete. *Construction and Building Materials*, Vol. 304, 2021, id. 124659.
[30] Zheng, Y., J. Zhuo, P. Zhang, and M. Ma. Mechanical properties and meso-microscopic mechanism of basalt fiber-reinforced recycled aggregate concrete. *Journal of Cleaner Production*, Vol. 370, 2022, id. 133555.
[31] Figiela, B., H. Šimonová, and K. Korniejenko. State of the art, challenges, and emerging trends: Geopolymer composite reinforced by dispersed steel fibers. *Reviews on Advanced Materials Science*, Vol. 61, 2022, pp. 1–15.
[32] Xu, Z., Z. Huang, C. Liu, X. Deng, D. Hui, Y. Deng, et al. Experimental study on mechanical properties and microstructures of steel fiber-reinforced fly ash-metakaolin geopolymer-recycled concrete. *Reviews on Advanced Materials Science*, Vol. 60, 2021, pp. 578–590.
[33] Xu, Z., J. Wu, M. Zhao, Z. Bai, K. Wang, J. Miao, et al. Mechanical and microscopic properties of fiber-reinforced coal gangue-based geopolymer concrete. *Nanotechnology Reviews*, Vol. 11, 2022, pp. 526–543.
[34] Adak, D., M. Sarkar, and S. Mandal. Structural performance of nano-silica modified fly-ash based geopolymer concrete. *Construction and Building Materials*, Vol. 135, 2017, pp. 430–439.
[35] Xu, Z., Z. Bai, J. Wu, H. Long, H. Deng, Z. Chen, et al. Microstructural characteristics and nano-modification of interfacial transition zone in concrete: A review. *Nanotechnology Reviews*, Vol. 11, 2022, pp. 2078–2100.
[36] Ismael, R., J. V. Silva, R. N. F. Carmo, E. Soldado, C. Lourenço, H. Costa, et al. Influence of nano-SiO2 and nano-Al2O3 additions on steel-to-concrete bonding. *Construction and Building Materials*, Vol. 125, 2016, pp. 1080–1092.
[37] Chu, H., Y. Zhang, F. Wang, T. Feng, L. Wang, and D. Wang. Effect of graphene oxide on mechanical properties and durability of ultra-high-performance concrete prepared from recycled sand. *Nanomaterials*, Vol. 10, 2020, id. 1718.
[38] He, S. and E.-H. Yang. Strategic strengthening of the interfacial transition zone (ITZ) between microfiber and cement paste matrix with carbon nanofibers (CNFs). *Cement and Concrete Composites*, Vol. 119, 2021, id. 104019.
[39] Alomayri, T. Performance evaluation of basalt fiber-reinforced geopolymer composites with various contents of nano $CaCO_3$. *Ceramics International*, Vol. 47, 2021, pp. 29949–29959.
[40] Ranjbar, N., S. Talebian, M. Mehrali, C. Kuenzel, H. S. Cornelis Metselaar, and M. Z. Jumaat. Mechanisms of interfacial bond in steel and polypropylene fiber reinforced geopolymer composites. *Composites Science and Technology*, Vol. 122, 2016, pp. 73–81.
[41] Xu, Z., Q. Liu, H. Long, H. Deng, Z. Chen, and D. Hui. Influence of nano-SiO2 and steel fiber on mechanical and microstructural properties of red mud-based geopolymer concrete. *Construction and Building Materials*, Vol. 364, 2023, id. 129990.
[42] Dişçi, E. and R. Polat. The influence of nano-CaO and nano-Al_2O_3 and curing conditions on perlite based geopolymer concrete produced by the one-part mixing method. *Construction and Building Materials*, Vol. 346, 2022, id. 128484.
[43] Sumesh, M., U. J. Alengaram, M. Z. Jumaat, K. H. Mo, and M. F. Alnahhal. Incorporation of nano-materials in cement composite and geopolymer based paste and mortar – A review. *Construction and Building Materials*, Vol. 148, 2017, pp. 62–84.
[44] Fang, G., Q. Wang, and M. Zhang. Micromechanical analysis of interfacial transition zone in alkali-activated fly ash-slag concrete. *Cement and Concrete Composites*, Vol. 119, 2021, id. 103990.
[45] Wang, X., Q. Zheng, S. Dong, A. Ashour, and B. Han. Interfacial characteristics of nano-engineered concrete composites. *Construction and Building Materials*, Vol. 259, 2020, id. 119803.
[46] Alomayri T., A. Raza, and F. Shaikh. Effect of nano SiO2 on mechanical properties of micro-steel fibers reinforced geopolymer composites. *Ceramics International*, Vol. 47, 2021, pp. 33444–33453.